N94-11312

(NASA-CR-193283) MODELS OF
NEPTUNE'S SMOOTH RECURRENT RADIO
EMISSION Final Report, 4 June 1992
- 9 Jul. 1993 (Radiophysics) 14 p

Unclas

G3/93 0175332

NASA-CR-193283

Radiophysics, Inc.
Boulder, CO. 80301

Contract NASW-4697, Smooth Recurrent Emission: Final Report

IN-93-CR
175332

1. Work Originally Proposed

The goal is to locate radio sources and determine emission characteristics: mode, intensity, emission angle, and degree of polarization. The analysis compares observations of power and degree of circular polarization to modeled values of these quantities. In addition to the geometry of the spacecraft relative to a radio source with postulated location and emission beam, the simulation includes the response of the Planetary Radio Astronomy (PRA) instrument to an incident wave of defined but arbitrary polarization. Modeled shape and orientation of the incident polarization ellipse depends on the angle between the wave vector and the direction of the magnetic field at the radio source. The link between radio emission characteristics and source location is provided by a model of Neptune's magnetic field. The proposed simulations of the time variation of intensity and polarization are based on an offset tilted dipole model of Neptune's magnetic field: the OTD2 model [*Ness* 1990].

2. Dipole and Multipole Magnetic-Field Models.

RPI's proposals were submitted in June, 1991. At the end of October, 1991, the spherical harmonic model of Neptune's field was published [*Connerney et al.*, 1991]. In preparation for the NDAP work, we explored differences between various offset tilted dipole models and the O8, 15-coefficient spherical harmonic model. A report on our findings concerning magnetic-field models was submitted January 11, 1993, addressed to Jay Bergstrahl. We found that the radio sources lie in a part of Neptune's magnetosphere where the O8 model is very different from any dipole model. Figure 1 illustrates the situation. The right side illustrates the dipole-based analysis described in this report. Radio sources lie on axial-symmetric surfaces defined by the constant magnetic-field intensity that corresponds to the electron cyclotron frequency. Field direction is determined by magnetic latitude. The left side of the figure represents one longitude in the O8 model field. Each longitude is different. Additional poles create strong gradients of field strength and direction. Radio sources occur with instability in the distribution and motion of electrons, and this must be strongly affected by the structure of the field. The cyclotron maser mechanism of radio emission is limited by the ratio of plasma frequency to cyclotron frequency; this ratio must change rapidly where the constant-field surface is strongly distorted. Propagation of the radio wave also is dependent on this ratio and on field direction. For all of these reasons, the differences between the O8 model and the OTD2 (offset tilted dipole) model strongly affect the analysis of radio data. Because of the important influence of the magnetic-field model, the present report on the contracted work based on the OTD2 model emphasizes methods of analysis rather than specific results.

Before comparing simulations of the wide-cone and filled-cone models, we discuss the instrument response. Quantitative modeling of instrument response is an important difference between the studies of PRA data that have been published.

2.1 *Instrument Response* The effective antenna plane or electric plane of PRA's orthogonal dipole antennas is tilted about 20° to the physical antenna plane. Apparent fractional polarization AFP vanishes for a source in the direction of the electric plane [*Warwick et al.* 1977]. The response to a low-frequency wave that is completely circularly polarized (true polarization ratio TPR = ± 1) was described by *Warwick et al.* [1977], *Daigne and Ortega-Molina* [1984], and others. The apparent polarization of such a wave will, in general, be reduced relative to the polarization of the incident wave. A special case occurs when the wave arrives along one pole of the electric plane and retains its circular polarization (the instrument senses AFP = TPR = 1). Along the opposite antenna pole, sense of circular polarization is reversed (AFP = -TPR = -1; the apparent polarization sense is then labeled "false". At each direction away from the poles, response to elliptical polarization depends on orientation of the polarization ellipse relative to the antennas. Each of six contour plots in Figure 4 of *Sawyer et al.* [1991] shows how response to waves of a certain polarization state depends on direction of arrival. Another special case that is less known *enhances* circular polarization for certain directions and orientations of the instrument . An occasion when such enhancement must have occurred at Neptune will be described later. Polarization enhancement occurs when the major axis of the polarization ellips is in the meridian plane of the antennas and nearly normal to the antenna electric plane. Then the component of the wave electric vector parallel to the major axis is foreshortened and the apparent polarization ellipse becomes more nearly circular.

At a distance from the planet greater than about 15 R_N the angular size of the radio surface is small. Waves that reach the antennas from any source on the surface have approximately the same direction in the antenna coordinate system. Then the instrumental response to waves from different sources depends only on their differing polarization. This arises from different emission angles corresponding to different magnetic-field direction at various source sites. When Voyager is closer to the planet, the arrival direction of waves from sources at different parts of the source surface can be different and this affects the instrumental response. Figure 2 of *Sawyer et al.* [1991] shows projections of a source surface of Uranus onto the antenna coordinate surface at distances of 34 and 7.4 R_U. At Neptune, for frequencies lower than 270 kHz, Voyager passes inside the source surfaces. Seen from within, the source surface fills all directions.

Figure 1 is plotted in the same antenna coordinates as Figure 2 of *Sawyer et al.* [1991], but while the earlier figure outlines the source surface at two different times, Figure 1 represents a sequence of 15 different times. It attempts to represent at each time the angular size and orientation of the source surface relative to the electric plane. To avoid overlap, only the magnetic poles, N and S, are shown, with a line (the dipole axis) connecting them. The magnetic poles on the 154.8 kHz surface are shown during the first half of day 237. Between 0200 and 0600 SCET the electric plane crosses the source surface. (Voyager was inside the surface between 0329 and 0412.) From 0600 to 1000 SCET all points on the source surface are near a pole of the antenna plane, the one that makes AFP "false". In this period the expected instrumental effect is slight reduction and reversal of circular polarization. After 1005, all radio sources are "true". They are close to the antenna plane , which in general reduces apparent polarization. However, they are near the meridian plane at $\phi = 180^{\circ}$, and meet some of the conditions for instrumental enhancement of polarization. Information on source location derived from the time of the apparent polarization reversal will be described below.

3. Numerical Simulation

The observed smooth recurrent emission (SRE) at frequencies near 150 kHz includes right-hand polarized (RHP) emission that repeats predictably, and LHP spikes that precede the RHP emission, showing more variation from one cycle to another. The dominant RHP emission occurs at the phase when Voyager is in the northern magnetic hemisphere. At higher frequencies, near 500 kHz, LHP emission is observed at this phase, with RHP emission following. The time variation of power and polarization was simulated for six cycles of data (102 hours). Simulations at two frequencies 154.8 kHz and 462.0 kHz are illustrated.

a. Snapshot maps. Surveys of the entire source surface are made at key times such as peaks of emission and polarization. At each point on the latitude-longitude grid on the constant-frequency surface we calculate the radio-emission characteristics imposed by the relation of the source to the magnetic field and to the PRA antennas. These characteristics are: the required emission angle (the angle between the magnetic-field direction at the source and the vector from source to Voyager); the sign of the field gradient along the source-Voyager vector; the minimum distance R_{min}, from the planet center to the line of sight; the source height R_{sp}, relative to the planet center; the apparent fractional polarization; and the power. The significance of these quantities is described briefly. The emission angle is expected to be a non-varying characteristic of a given source at a given frequency. It determines much of the apparent time variation related to Voyagr's changing position relative to the radio source. A nonpositive gradient of field magnitude along the propagation path at the source is a criterion for extraordinary-mode (X mode) propagation (the frequency must exceed the X-mode cutoff frequency). If the source is not occulted by the planet, the value of R_{min} must exceed the planet radius. If the source is not occulted by the ionosphere, R_{min} must exceed the ionospheric height at which the plasma frequency in the topside ionosphere equals the working frequency. The distance R_{sp} from planet center to source can be compared to the height of the ionosphere to estimate whether the ratio f_p /f_c is small enough for generation of emission by the mechanism known as the cyclotron maser instability (CMI). Models of electron density in the ionosphere and magnetosphere serve to relate f_p to altitude.

The snapshot maps are used to identify visible source locations from which apparent polarization matches observed polarization at a given time. Initially chosen key times are: times of maximum emission, of maximum apparent polarization, times when emission first appears or is cut off, and times when a sudden reversal of sense of polarization suggests that the source is in the antenna electric plane. Characteristics are mapped also at times when no emission was seen at Voyager. Thus the snapshot maps locate possible sources and eliminate other source locations without assumptions that limit the results. Approximately 20 sets of snapshot maps were calculated and plotted at various frequencies and times.

b. Simulation of time variation. After candidate source locations are selected with the aid of the snapshot maps for key times, each location can be tested over the entire data period. For a source or limited set of sources, a simulation of time variation of power and polarization is compared to the same quantities measured by the PRA instrument. Discrepancies between the modeled values and the observed values are noted. The free parameters: emission angle and beam width, power, latitude and longitude are varied in a search for better agreement with the data and for insight into the effect of these quantities on the observed emission. Except for averaging, the data are used as they are received. Rather than "correcting" or "cleaning" the data, we estimate the background noise, then add it to the simulation. Similarly, we determine the instrument response, then include it in the simulation. The advantage is that only the models and not the data are affected by estimates of these sometimes uncertain quantities.

4. Results

a. General characteristics of the data. The observed degree of polarization is positively correlated with intensity or power. This indicates that the weakly-polarized background noise usually predominates over the planetary emission. This interpretation leads to the estimate that circular polarization of at least 90% would be observed much of the time if the sources were stronger or closer.
Also apparent is an expected dependence of observed degree of polarization on source location with respect to the antennas: when the entire radio planet lies far from the antenna electric plane, strong polarization is observed.

Much of the time at Neptune, however, the radio planet lies close to the antenna electric plane. On one occasion, the observed circular polarization is nevertheless strong. In Figure 2 the 154.8 kHz source surface is shown very close to the electric plane at 1005 and 1006 SCET on day 237. Shortly thereafter, degree of polarization of -0.96 is observed when the instrument response to a circularly polarized wave would be -0.5, or even closer to 0. Values of apparent polarization at Neptune differ from those at Uranus, where the radio planet was usually far from the antenna electric plane and the apparent polarization was that expected for a circularly polarized incident wave.

b. Analysis: filled cone.
154.8 kHz. Simulation of the time variation of power and polarization at 154.8 kHz confirmed that the phase, duration, power, and polarization sense are successfully modeled in a dipole magnetic field with a filled emission beam from midlatitude conjugate sources that are distributed over a limited range of longitude. The data require sources in the magnetic west longitude range -45° to 85° and allow sources in the range -175° to 85°. A dipole magnetic model leads to the expectation of longitudinal symmetry, but the small-scale structure of the spherical harmonic model suggests localized radio sources. The simulated emission fails to attain the observed degree of left-hand polarization when modeled power matches observed power. The modeled value is only about 0.80 when the observed value is sometimes 1.0. The modeled degree of right-hand polarization also falls short near closest approach. Voyager was inside the 154.8 kHz source surface from 0339 to 0410 SCET (SpaceCraft Event Time). No X-mode emission is modeled during this period. (Emission at 0420 SCET was identified as electron-cyclotron harmonic emission [*Barbosa et al.* 1990; *Sawyer et al.* 1990].) After a change in sense of polarization accompanying a sharp decrease in power at 0335, emission continues well above background. This emission must be O-mode. Latitude $\pm 47^{\circ}$ corresponds to L = 3.4 on the 154.8 kHz surface. A filled cone fit the Neptune data with 5 adjustable parameters: source magnetic latitude, two limits of longitude, emission cone angle, and width.

As the electric plane sweeps northward across the source surface between 0200 and 0600 SCET, AFP changes from "true" to "false" and from RHP to LHP. Changing orientation of the source surface and its increasing angular size add complexity to the spatial polarization pattern as Voyager approaches the planet. The observed 0237 SCET polarization reversal requires a source at magnetic latitude 30° or lower, with corresponding $L < 2$. This discrepancy with results based on phase may reflect the inadequacy of the dipole magnetic model.

462 kHz. The phase and duration of SRE is different at higher frequency. In a dipole field, the emission at higher frequency can be modeled with a filled beam from conjugate sources at latitude ± 25° (L = 1.22). The allowed longitude range is -145° to 180° and the required range is 0° to 80°. Figures 4, 5, and 6 show that the simulation reproduces the phase, duration, and polarization of the recurrent emission features.

c. Analysis: Wide-cone.
Ladreiter et al. [1991] also chose midlatitude conjugate sources to explain low-frequency SRE. We follow *Carr et al.* [1993] in referring to these authors as *LLRR*. They assumed that the emission angle must be wide, and chose values of 80° in the southern hemisphere and 60° in the northern hemisphere. They distributed the sources in limited longitude ranges, different in each hemisphere. Different L-shells in the range 6 to 10 are invoked to explain different data. We tried various values and found that the phase and duration of emission at 154.8 kHz is fit best by sources at latitude ±66° (L = 10). *LLRR* claim that the same sources account for both SRE and HLE. We modified the computer program that simulates time variation of power and polarization to include the additional parameters required by *LLRR*. Different longitude ranges and different cone angles in the two hemispheres add 3 free parameters to the wide-cone model, making a total of 8. In spite of this additional freedom, thewide-cone model fails to fit phase and duration of the low-frequency SRE as faithfully as the filled-cone model of*Sawyer et al.* [1991]. Moreover, the degree of polarization is much less than observed: the wide-cone predicts degree of polarization < 0.3 when a filled cone predicts 0.8 and 1.0 is observed. Wide-cone sources at lower latitude successfully simulate HLE as LHP emission at 0320 SCET on day 237, but at the expense of filling in the emission gap. *LLRR* fit HLE at 39.6 kHz with sources on L = 6, and in a separate analysis choose sources at L = 10 to fit the emission gap at 154.8 kHz. Comparison of results of two methods using the same magnetic model shows the usefulness and importance of considering all the data, including both power and polarization, in a single analysis.

Rather than pursue the differences between the dipole-based models, we ask how, in view of the great differences between dipole and spherical harmonic magnetic models, the OTD model can simulate the results as well as it does. The answer may be that the simulations fit only the phase and duration of the recurrent emission, with essentially independent solutions at each representative frequency. It remains to be seen whether discrepancies disappear when simulations are based on a more complex magnetic-field model.

RECOMMENDATIONS

1. Results of analysis of radio data depend on the magnetic model in a fundamental way and a dipole magnetic model fails to describe the magnetic environment of Neptune radio sources. It is important to use the best magnetic model available, and to be aware of its shortcomings in regard to representation of radio emission and propagation.

2. It is possible to consider quantitatively the response of the PRA antennas to the individual characteristics of an incident radio wave and it is important to do so.

3. We should try to take into account the effects of polarization transfer between source and antennas -- the "limiting polarization region" for a radio wave--in order to get a more accurate description of the radio wave incident on the PRA antennas.

4. The complexity of even the O8 magnetic model suggests that there may be several locations where field direction would permit a match of phase and duration at a single frequency. We have gone beyond accepting a solution that fits one frequency at one time, and need to find ways to relate the data at all frequencies in proposing and testing candidate source locations and emission characteristics.

REFERENCES

Barbosa, D.D., W.S. Kurth, I.H. Cairns, D.A. Gurnett, and R.L. Poynter, Electrostatic electron and ion cyclotron harmonic waves in Neptune's magnetosphere, *Geophys. Res. Let., 17,* 1649-1652, 1990.

Carr, T.D. and S. Gulkis, The auroral kilometric radiation from Uranus and its magnetospheric implications, pp.223-235 in *Planetary Radio Emissions II,* H.O. Rucker, S.J. Bauer, and B.M. Pedersen (eds.); Proc. of the Second International Workshop on Planetary Radio Emissions, Graz, Austria, Sept., 1987.

Carr, T.D., Liyun Wang, and F. Reyes, Voyager radio investigations of Neptune and Uranus, *NASA grant no. NAGW-2410,* February 23, 1993.

Connerney, J.E.P., M. Acuna, and N. Ness, The magnetic field of Neptune, *J. Geophys. Res., 96,* 19,023-19,042, 1991.

Daigne, G. and A. Ortega-Molina, On polarization transfer in an inhomogeneous birefringent medium, *Astron.Astrophys., 133,* 69-76, 1984.

Ladreiter, H.P., Y. Leblanc, G.K.F. Rabl, and H.O. Rucker, Emission characteristics and source location of the smooth Neptunian kilometric radiation, *J.Geophys.Res., 96,*

Ness, N.F. *private communication,* 1990.

Sawyer, C.B., K.L. Neal, and J.W. Warwick, Polarization model applied to Uranian radio emission, *J.Geophys.Res., 96,* 5575-5590, 1991.

Sawyer, C., J.W. Warwick, and J.H. Romig, Smooth radio emission and a new emission at Neptune, *Geophys. Res. Let., 17,* 1645-1648, 1990.

Warwick, J.W., D.R. Evans, G.R. Peltzer, R.G. Peltzer, J.H. Romig, C.B. Sawyer, A.C. Riddle, A.E. Schweitzer, M.D. Desch, M.L. Kaiser, W.M. Farrell, T.D> Carr, I. de Pater, D.H. Staelin, S.G.Gulkis, R.L. Poynter, A. Boischot, F. Genova, Y. Leblanc, A.Lecacheux, B.-M. Pedersen, and P. Zarka, Voyager planetary radioastronomy at Neptune, *Science, 246,* 1498-1501, 1989.

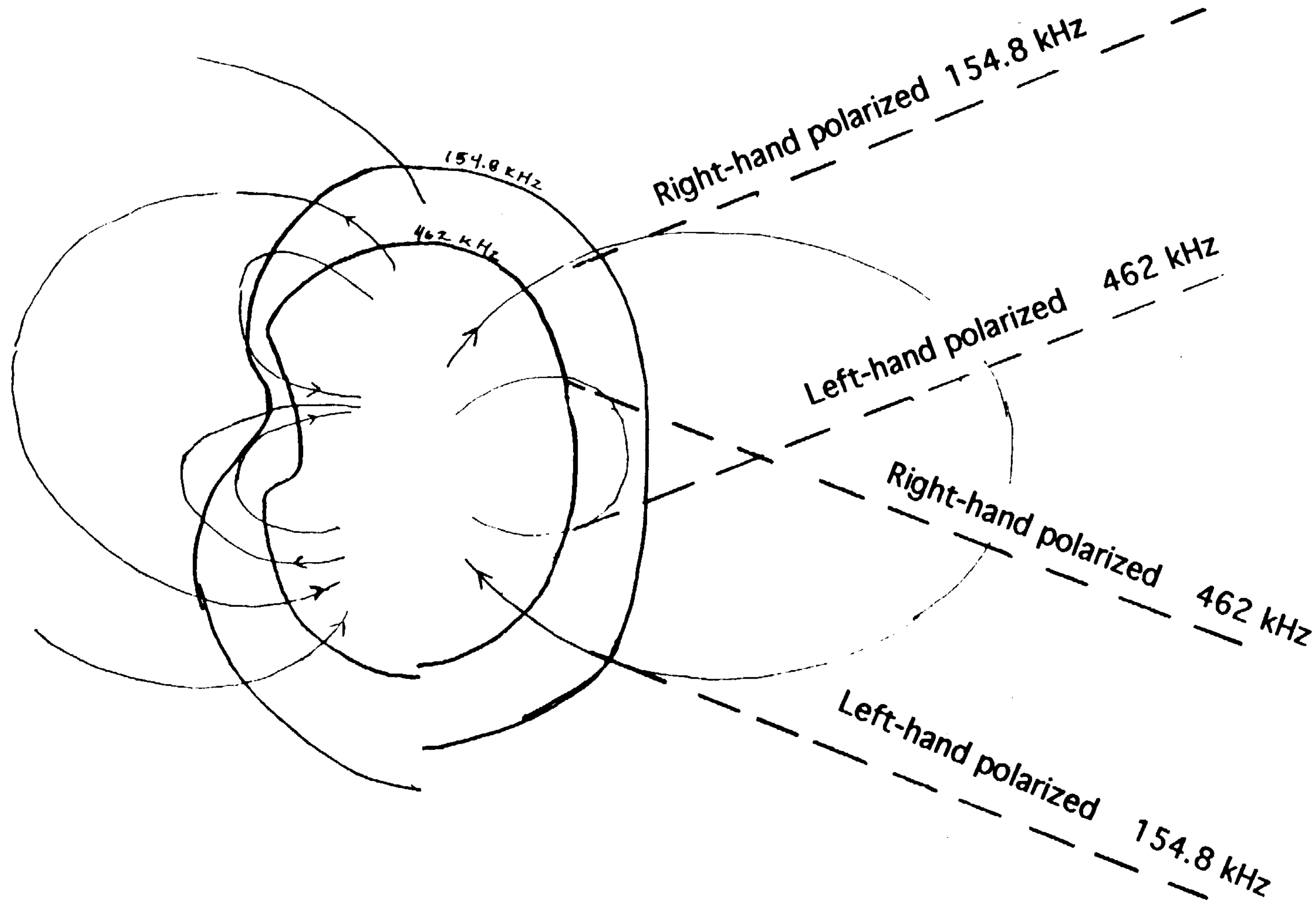

Figure 1. Dipole and O8 magnetic-field models. Heavy curves show meridional sections of constant-field surfaces. Each surface is the locus of radio sources of emission at the corresponding electron cyclotron frequency. Lighter continuous curves are representative magnetic field lines. Dashed straight lines represent lines of sight from radio sources. Modeled radio emission is emitted in a cone, wide and hollow, or narrow and filled, centered on these or similar lines.

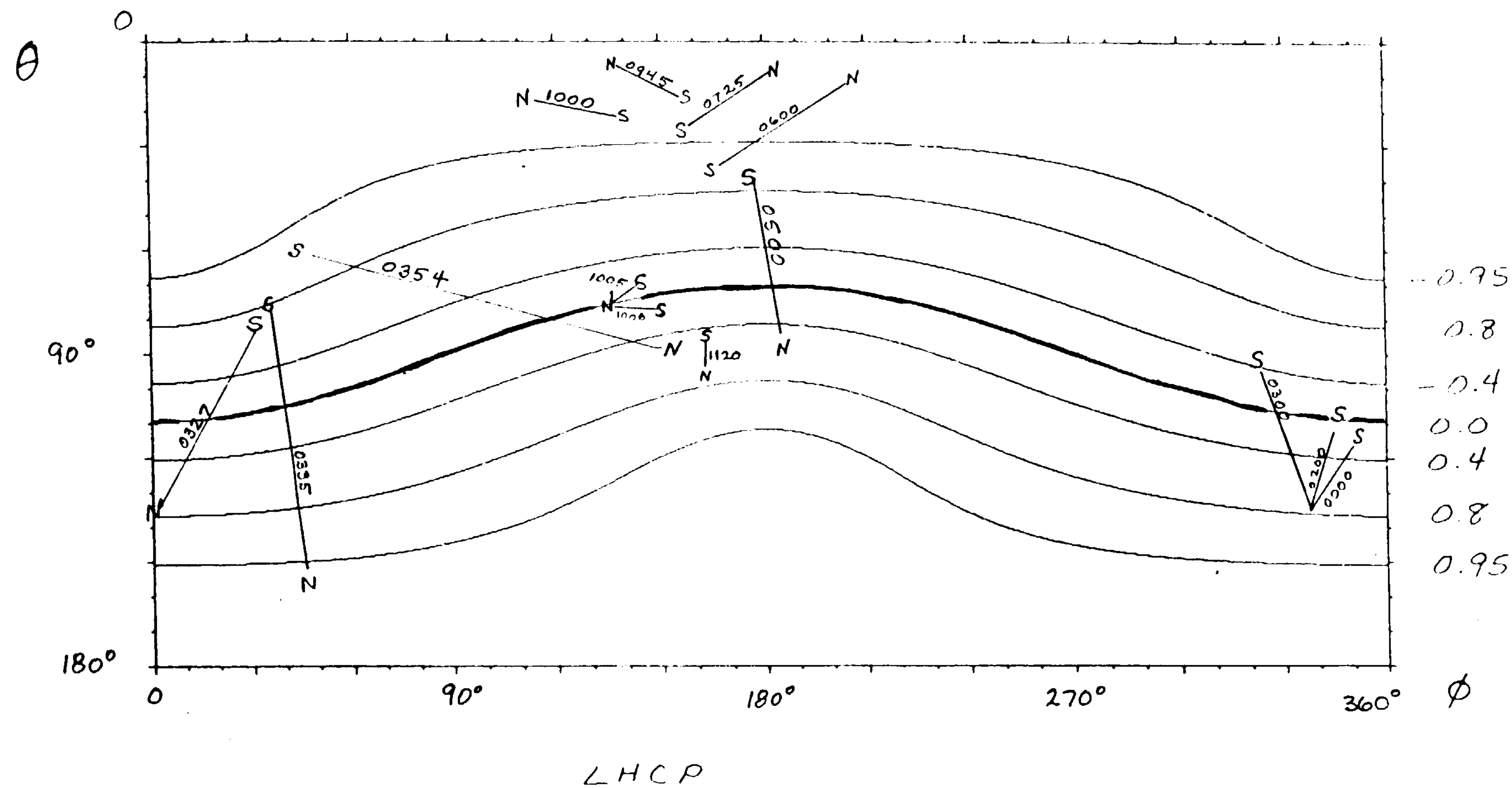

Figure 2. Antenna coordinates of the 154.8 kHz surface defined by the OTD2 magnetic model. The surface as seen from Voyager at a sequence of times during the first half of day 237 is represented by the north and south poles, labeled N and S, connected by the dipole axis. The abscissa f is the angle in the antenna plane from a radius midway between the antennas, and the ordinate q is the angle from the axis normal to the antenna plane (see Fig. 1 of *Sawyer et al.* [1991]). Voyager is within the 154.8-kHz surface from 0329 to 0412 SCET. Apparent polarization AFP is "false" at all points on the source surface from 0600 to 1000 SCET. The time between 0200 and 0600 at which the change from "true" to "false" occurs depends on frequency and source location. The subsequent change from "false" to "true" occurs over the entire surface within a few minutes near 1005 SCET. Afterward the source surface lies near the meridian plane at f = 180°, and close to the electric plane.

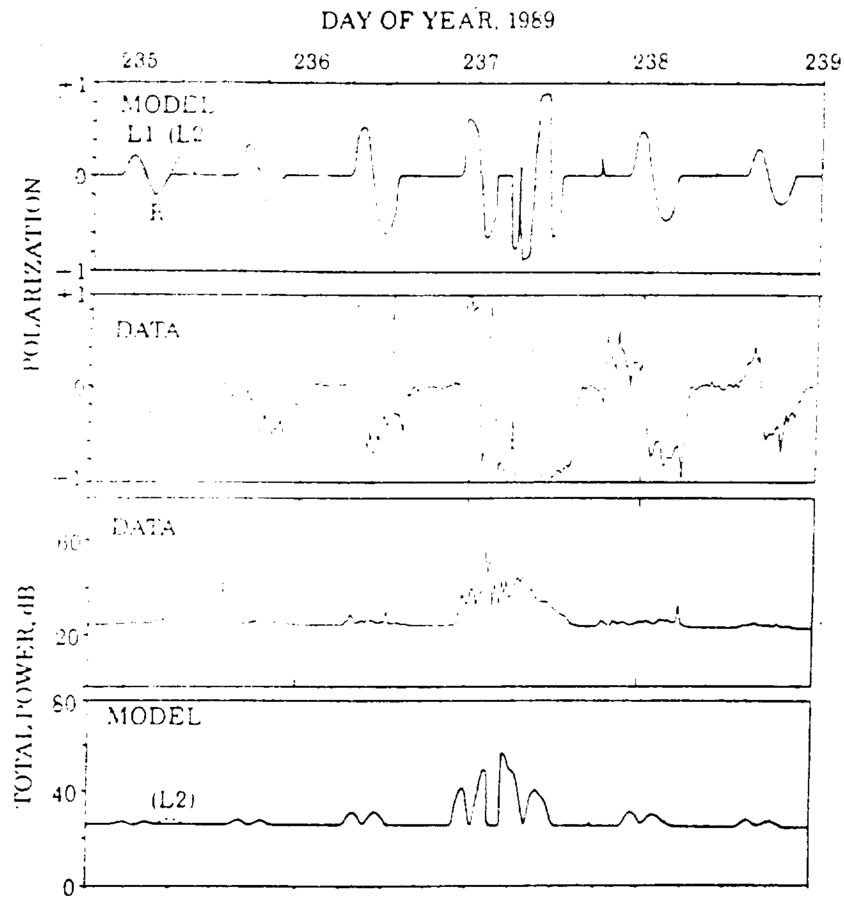

Fig. 3. Observed and simulated total power and degree of circular polarization at frequency 154.8 kHz. A new simulation with more restricted range of source longitude is essentially identical to this one, taken from *Sawyer et al.* [1990]. The dipole-based model fits phase and sense of polarization.

REPORT DOCUMENTATION PAGE

Form Approved
OMB No. 0704-0188

1. AGENCY USE ONLY (Leave blank)	2. REPORT DATE	3. REPORT TYPE AND DATES COVERED
	July 9, 1993	Final June 4, 1992-July 9, 1993

4. TITLE AND SUBTITLE
Models of Neptune's Smooth Recurrent Radio Emission

5. FUNDING NUMBERS
NASW-4697

6. AUTHOR(S)
Constance Sawyer

7. PERFORMING ORGANIZATION NAME(S) AND ADDRESS(ES)
Radiophysics, Inc.
5475 Western Ave
Boulder, CO 80301

8. PERFORMING ORGANIZATION REPORT NUMBER

9. SPONSORING/MONITORING AGENCY NAME(S) AND ADDRESS(ES)
NASA Headquarters
Washington, DC 20546

10. SPONSORING/MONITORING AGENCY REPORT NUMBER

11. SUPPLEMENTARY NOTES

12a. DISTRIBUTION/AVAILABILITY STATEMENT

12b. DISTRIBUTION CODE

13. ABSTRACT (Maximum 200 words)

Models of Neptune's Smooth Recurrent Radio Emission

The quantitative response of the PRA instrument to a wave with polarization ellipse of arbitrary shape and orientation, arriving at the antennas from any direction, can be determined. We use this capability to model the time variation of intensity and circular polarization over a range of radio frequencies for proposed radio-source locations and emission characteristics at Neptune. At frequencies below 400 kHz the observed variation of intensity, polarization, and phase are closely simulated in an offset tilted dipole magnetic field by conjugate sources at midlatitude with filled emission cones. The phase of emission at higher frequencies is reproduced by sources at lower latitude. Modeled wide-cone emission does not reach the spacecraft at the observed phase nor have the polarization sense observed before closest approach. We present source-surface maps of apparent polarization for the period before closest approach, when instrumental response is especially sensitive to source location. The method is capable of extension to more realistic models of the magnetic field.

14. SUBJECT TERMS
Neptune radio emission, instrumental response, quantitative measure of polorization, radio-source location.

15. NUMBER OF PAGES
13

16. PRICE CODE

17. SECURITY CLASSIFICATION OF REPORT	18. SECURITY CLASSIFICATION OF THIS PAGE	19. SECURITY CLASSIFICATION OF ABSTRACT	20. LIMITATION OF ABSTRACT
Unclassified	Unclassified	Unclassified	UL

NSN 7540-01-280-5500

Standard Form 298 (Rev. 2-89)
Prescribed by ANSI Std. Z39-18
298-102